ANALYSIS OF DIRECTIONAL DATA

Since this distance is proportional to $|\theta_i - \tilde{\theta}|$ it is the equivalent of minimizing the sum

$$\text{minimize} \sum_{i=1}^{n} |\theta_i - \tilde{\theta}|, \tag{9.22}$$

which we know gives the median of the θ_i data set. Similarly, a LMS mode estimate can be found by determining the midpoint of the shortest arc containing $n/2 + 1$ points. Again, this would involve sorting the directions first, possibly after doubling orientations.

Example 9–4. Consider the wind directions

$$\theta_i : 75°, 85°, 90°, 98°, 170° \quad \bar{\theta} = 100.7°.$$

The shortest arc over 5/2 + 1 = 3 points is located between 85° and 98° , giving the mode estimate $\hat{\theta} = 91.5°$. This estimate suggests that 170° is an outlier with respect to the rest of the atmospheric data.

Figure 9.3: The effect of outliers on the mean direction is most severe when the outlier is orthogonal to the bulk of the data directions. Headed vectors represent the mean resultants.

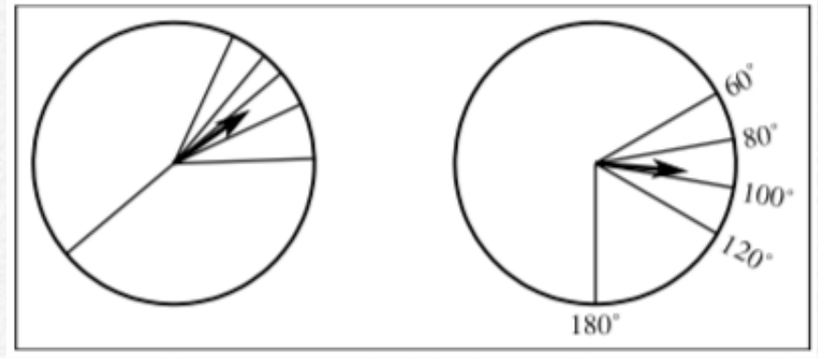

9.1.6 Data with length and direction

In the analysis so far we have only considered the direction (or orientation) of a feature and not its length. However in many cases, such as fracture data or fault traces, the features will have very different lengths. The analysis described above, when applied to such data, would give both a one km long and a 100 km long fault the same weight, which may not be appropriate. We can account for this bias by weighing the directions by the respective *lengths* of the features. By keeping track of the length of the faults (and not their numbers) per sector we can obtain a rose diagram that reflects the proportions of the various fracture directions. The rationale employed here is that large and/or long faults may be more representative of the tectonic stresses than a few short fractures. The rose diagram may then be normalized by the total length of the fractures to give overall proportions in percent.

ANALYSIS OF DIRECTIONAL DATA

Staying with fault strike data, it is clear that in many regions the faults are not entirely straight lines but may actually curve or bend. From a directional analysis point of view, such fractures must first be approximated by shorter straight line segments. It then becomes obvious that we must weigh the pieces by their lengths, otherwise the directional frequencies would depend on the number of pieces used. Fault traces must therefore be digitized prior to analysis on a computer. A typical fault trace is displayed in Figure 9.4. Depending on the angular width of the polar histogram,

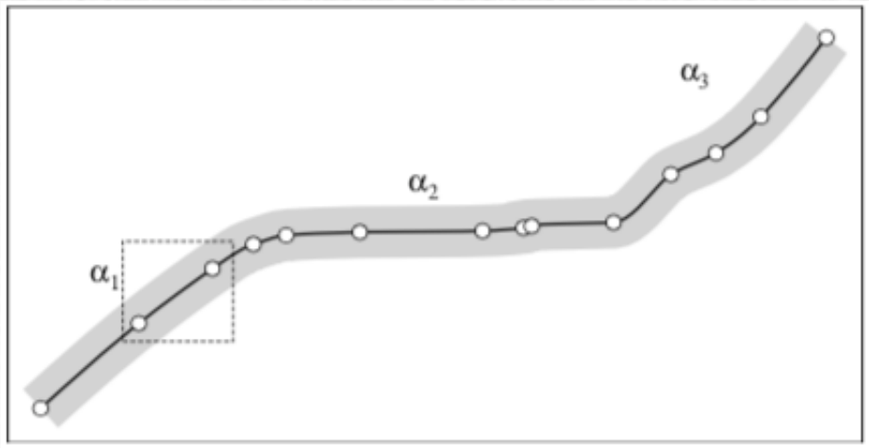

Figure 9.4: A digitized fault trace. Open circles indicate the digitized points. Digitizing too finely may lead to short-wavelength noise in the representation of the fault. Points within the dashed box are examined in Figure 9.5.

the digitized fault may end up in two bins corresponding to the orientations α_1 and α_2. We must also be aware of the fact that the digitizing process will introduce uncertainties in the digitized points. To see how this may affect the analysis, consider the line segment in Figure 9.5. We may assume that the exact position of each point is uncertain, here represented by the one-sigma uncertainty estimate s_r in radial position (gray circles) for each point. There are two points of interest here: First, the length of the segment, d, will have an uncertainty since it reflects a difference between two uncertain values. In Chapter 2, we found this to be

$$\Delta d = \sqrt{2} s_r, \quad d = d_0 \pm \Delta d, \tag{9.23}$$

assuming the uncertainties are *independent*. Second, we see that the direction (or orientation) α may be in error by ±Δα, given by

$$\Delta\alpha = \tan^{-1}(2s_r/d), \quad \alpha = \alpha_0 \pm \Delta\alpha. \tag{9.24}$$

Consequently, one should not digitize lines so frequently that Δα exceeds the desired polar histogram interval. For instance, if this interval is 10° then you are best served by making the average digitizing interval $d > 10 s_r$. Alternatively, one can *filter* the digitized track so that short-wavelength noise is smoothed out before binning the segments.

ANALYSIS OF DIRECTIONAL DATA

The length of all segments that have a direction within the width of a single bin is simply computed by adding up all the individual lengths. Note that since internal nodes are shared by adjacent line segments the uncertainty in the total length is independent of the number of line segments (e.g., Figure 2.2) and only depends on (9.23). However, the *sum* of the lengths of the individual segments will have an uncertainty that is cumulative since the segments are no longer connected. This method will provide a frequency distribution with error bars in which directions with many small segments will have higher uncertainty than directions with fewer and longer faults.

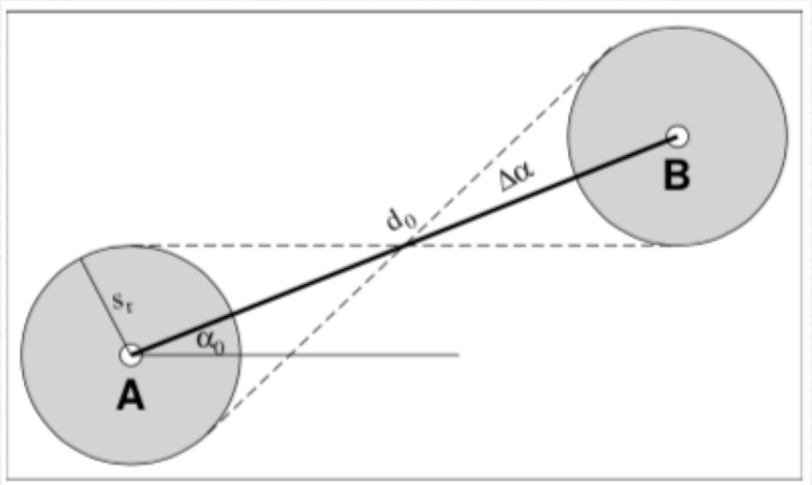

Figure 9.5: The uncertainty r_s in the locations of two digitized points (A and B) from Figure 9.4 introduce uncertainties Δd and $\Delta\alpha$ in the length (d_0) and orientation (α_0) of a line segment, respectively.

9.2 Spherical Data Distributions

The analysis of 3-D directions and orientations is an extension of the methods used for circular data. It is common to require that these 3-D vectors have unit lengths so that their endpoints all lie on the surface of a sphere with unit radius — hence the name spherical distributions. Similar to the 2-D case for circular data, there will be spherical data that only reflect orientations (i.e., *axes*) rather than directions. We need to use a 3-D Cartesian coordinate system to describe the unit vectors (Figure 9.6). Thus, any vector v is uniquely determined by the triplet (x,y,z). We could also use spherical angles θ (colatitude) and ϕ (longitude) to specify the vector direction, assuming the length $r = 1$.

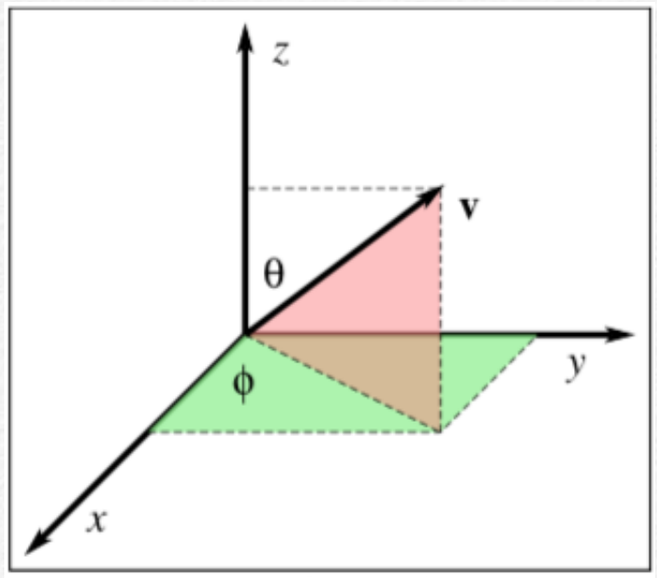

Figure 9.6: The relation between the Cartesian (x,y,z) and spherical (ϕ,θ,r) coordinate systems.

ANALYSIS OF DIRECTIONAL DATA

We relate the Cartesian coordinates and the spherical angles as follows:

$$\begin{aligned} x &= \sin\theta\cos\phi, \\ y &= \sin\theta\sin\phi, \\ z &= \cos\theta. \end{aligned} \qquad (9.25)$$

However, geological measurements like *strike* and *dip* are more commonly used than Cartesian coordinates and spherical angles and these follow their own convention. We define a new local coordinate system in which *x* points toward north, *y* points east, and *z* points vertically down (i.e., in order to maintain a right-handed coordinate system). In such a system, fault plane dips are expressed as positive angles. For the fault plane in Figure 9.7 we find that the angle *A* is the azimuth of the strike of the plane and *D* is the dip, measured positive down. The slip-vector *OP* is then given by its components

$$\begin{aligned} x &= -\sin A\cos D, \\ y &= \cos A\cos D, \\ z &= \sin D. \end{aligned} \qquad (9.26)$$

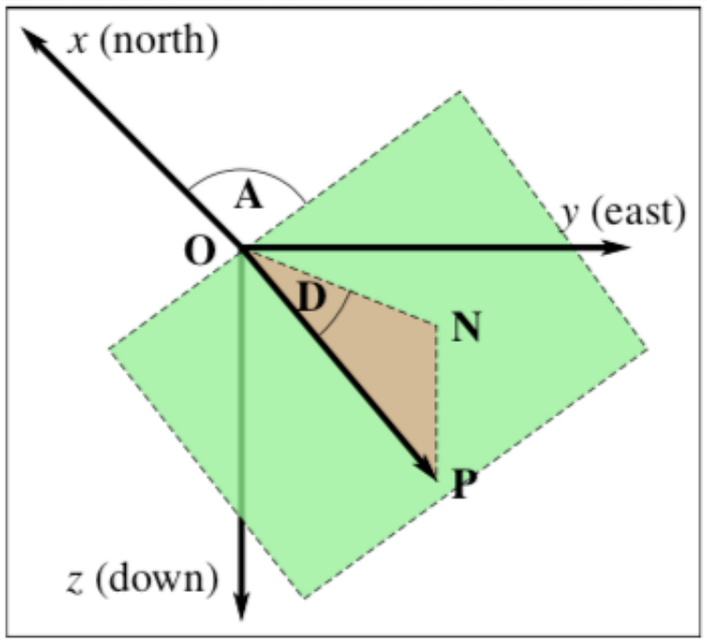

Figure 9.7: Local, right-handed coordinate system shows the convention used in structural geology. Here, *A* is the strike (measured from north over east) of the dipping plane (light green) and *D* is its dip, measured as the angle between the dip vector *OP* and its projection *ON* onto the horizontal *x* − *y* plane. The red plane containing the dip vector is orthogonal to the light green plane.

Once we have converted our (*A*, *D*) data to (*x*, *y*, *z*) we can compute such quantities as mean direction and spherical variance, which are simple extensions of the 2-D or directional analogs. The length of the resultant vector is simply

$$R = \sqrt{\left(\sum x_i\right)^2 + \left(\sum y_i\right)^2 + \left(\sum z_i\right)^2}, \qquad (9.27)$$

with the sum taken over all the *n* points. The resultant vector is usually normalized to give $\bar{R} = R/n$. The coordinates $\bar{x}$, $\bar{y}$ and $\bar{z}$ of the mean vector m are then obtained via

$$\bar{x} = \sum x_i/n, \quad \bar{y} = \sum y_i/n, \quad \bar{z} = \sum z_i/n, \qquad (9.28)$$

so that the mean slip-vector is given by its two components

$$\begin{aligned} \bar{D} &= \sin^{-1}\bar{z}, \\ \bar{A} &= \tan^{-1}(-\bar{x}/\bar{y}). \end{aligned} \qquad (9.29)$$

ANALYSIS OF DIRECTIONAL DATA

If all the vectors are closely clustered then the resultant R will approach n, but if the vectors are more randomly distributed then R will approach zero. As in 2-D, we can use R (or $\bar{R}$) as the basis for the *spherical variance*, s_s^2, given by

$$s_s^2 = (n - R)/n = 1 - \bar{R}. \tag{9.30}$$

9.2.1 Test for a random direction

We can perform simple hypothesis tests in a manner analogous to those we carried out for 2-D directional data. Unlike the case for 2-D we now require a *spherical* probability density function from which we can derive critical values for comparison with our observed statistics. In response to the need for 3-D statistical analysis, in particular for palaeomagnetic studies that started to explore "continental drift" in the 1950s, the famous British statistician Ronald Fisher developed a suitable theoretical distribution for spherical data. His probability density function has since been called the *Fisher* distribution on a sphere and is given by

$$P(\mathbf{x}) = \frac{\kappa}{4\pi \sinh \kappa} e^{\kappa(\mathbf{x}\cdot\boldsymbol{\mu})}, \tag{9.31}$$

where the dot product between the mean direction $\boldsymbol{\mu}$ and any other direction $\mathbf{x}$ equals the cosine of the angle ψ between them, κ is the precision parameter similar to the one we encountered for the von Mises distribution on the circle, and sinh is the *hyperbolic sine* function (which is needed to ensure the cumulative distribution of $P(\mathbf{x})$ over the unit sphere equals one).

Fisher showed one can estimate κ from the sample, provided $n > 7$ and $\kappa > 3$. The estimate is then given by

$$k \approx \kappa = \frac{n-1}{n-R}, \tag{9.32}$$

but more accurate tables also exist (e.g., Table A.18) which solve (A.3).

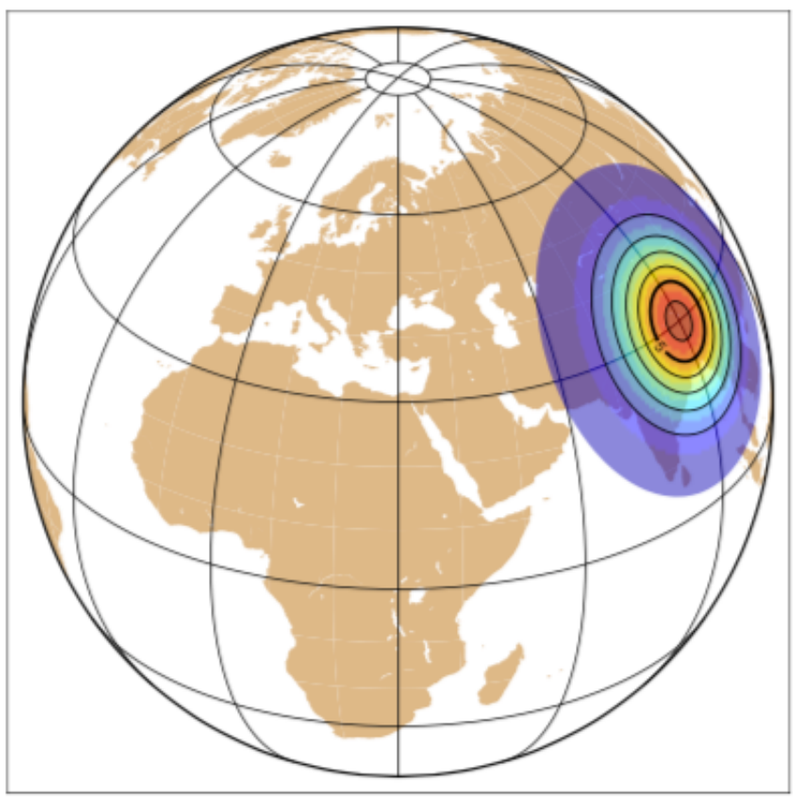

Figure 9.8: Well-focused Fisher distribution on a sphere, centered on a point in northern India, with κ = 40.

ANALYSIS OF DIRECTIONAL DATA

Testing a spherical distribution for randomness follows the same approach used for directional data: We must first evaluate $\bar{R}$, the mean resultant. Then, we state the null hypothesis to be

$$H_0 : \kappa = 0 \quad H_1 : \kappa > 0. \tag{9.33}$$

As before, this test is executed by establishing critical values of $\bar{R}$ given the prescribed level of confidence, α. Table A.19 shows such critical $\bar{R}$ values for selected values of α and n.

Example 9–5. Let us examine a set of palaeomagnetic measurements. We have been given six measurements of *declination* and *inclination*, reported as

Dec	105°	130°	115°	120°	118°	145°
Inc	40°	49°	57°	32°	55°	45°

First, we note that a dip-vector specified by strike A and dip D is not using the same geometry as a magnetic field vector given by its magnetic declination D and inclination I. Because the projection of the dip-vector onto the horizontal plane is 90° away from the strike, we must use a slightly modified conversion suitable for magnetic vectors to obtain the Cartesian coordinates:

$$\begin{aligned} x &= \cos D \cos I, \\ y &= \sin D \cos I, \\ z &= \sin I. \end{aligned} \tag{9.34}$$

We convert the n = 6 observed declinations and inclinations to x, y, z and find

x	−0.20	−0.42	−0.23	−0.42	−0.27	−0.58	$\bar{x}$	−0.354
y	0.74	0.50	0.49	0.73	0.51	0.41	$\bar{y}$	0.564
z	0.64	0.75	0.84	0.53	0.82	0.71	$\bar{z}$	0.715

ANALYSIS OF DIRECTIONAL DATA

Computing the mean direction and resultant gives

$$\bar{I}_1 = \sin^{-1}\bar{z} = 45.7^\circ, \tag{9.35}$$

$$\bar{D}_1 = \tan^{-1}\bar{y}/\bar{x} = 122.1^\circ, \tag{9.36}$$

$$\bar{R}_1 = \frac{1}{6}\cdot 5.86 = 0.977, \tag{9.37}$$

$$k_1 = \frac{6-1}{6-5.86} = 35.7. \tag{9.38}$$

It is evident that our distribution has a clear preferred direction since k_1 is so large (the critical $\bar{R}$ for $\alpha = 0.05$ is only 0.642).

9.2.2 Test for a specific direction

Often, we will be interested in testing whether the observed mean direction equals a prescribed direction, given the uncertainties due to random errors. As for circular data, such tests are best performed by constructing the α confidence region around the mean direction. This statistic is based on the Fisher distribution and gives a spherical cap radius for a *cone of confidence* around the mean direction. As usual, this radius, δ, is a function of both the confidence level α and R. We find

$$\delta_{1-\alpha} = \cos^{-1}\left\{1 - \frac{n-R}{R}\left[\left(\frac{1}{\alpha}\right)^{\frac{1}{n-1}} - 1\right]\right\}. \tag{9.39}$$

This fairly complicated expression simplifies considerably if we assume (or actually know) that $k > 7$ and standardize our tests for $\alpha = 0.05$. Then,

$$\delta_{95\%} \approx 140^\circ/\sqrt{kn} \tag{9.40}$$

given in spherical degrees. We may now say that there is a 95% probability that the true mean direction lies within the cone of confidence specified by the angular radius $\delta_{95\%}$.

ANALYSIS OF DIRECTIONAL DATA

The application of the cone of confidence is more involved than for circular data since we cannot directly compare the two angular measures defining the mean direction (e.g., strike, dip) to the comparable quantities of a specific direction to be tested, here called $\hat{\mathbf{v}}$. Instead, we need to utilize their Cartesian vector representations. The procedure is still relatively straightforward:

1. State the null hypothesis that the unit vectors are the same, i.e., $H_0 : \hat{\mathbf{m}} = \hat{\mathbf{v}}$.
2. Take the dot-product of the mean unit vector with the test unit vector, i.e, $c = \hat{\mathbf{m}} \cdot \hat{\mathbf{v}}$.
3. Since a dot product gives the cosine of the spherical angle between two vectors we find this distance to be given by $\psi = \cos^{-1} c$.
4. If ψ exceeds $\delta_{95\%}$ then $\hat{\mathbf{v}}$ is outside the cone of confidence and we can reject the null hypothesis; otherwise we must reserve judgment.

For other levels of confidence we would substitute the general radius specified in (9.39).

Example 9–6. Given the data we just analyzed we want to test if the mean vector we found is compatible with an hypothesis that says the inclination should be 45° and the declination should be 120°. First, we find the unit vector pointing in the same direction as the mean resultant, m. This vector is

$$\hat{\mathbf{m}} = \frac{\mathbf{m}}{|\mathbf{m}|} = \frac{(-0.354, 0.564, 0.715)}{\sqrt{0.354^2 + 0.564^2 + 0.715}} = (-0.3621, 0.5770, 0.7321). \tag{9.41}$$

We evaluate the test vector to be

$$\hat{\mathbf{v}} = (\cos 120^\circ \cdot \cos 45^\circ, \sin 120^\circ \cdot \cos 45^\circ, \sin 45^\circ) = (-0.3536, 0.6124, 0.7071). \tag{9.42}$$

Hence, the angle between the mean and the test vector is given by their dot product:

$$\psi = \cos^{-1}(0.3621 \cdot 0.3536 + 0.5770 \cdot 0.6124 + 0.7321 \cdot 0.7071) = \cos^{-1}(0.9990) = 2.53^\circ. \tag{9.43}$$

To determine the radius of the 95% confidence cone we use (9.40) and find

$$\delta_{95\%} \approx 140^\circ / \sqrt{35.7 \cdot 6} = 9.6^\circ. \tag{9.44}$$

This means that the true population mean direction probably (i.e., with 95% level confidence) lies within a spherical cone of radius 9.6° centered on the observed mean direction. Clearly, our test vector v also lies inside this cone. Therefore, we cannot reject the null hypothesis that they point in the same direction.

ANALYSIS OF DIRECTIONAL DATA

A.8 Relationship Between κ and $\bar{R}$ for 2-D Directional Data

Given a mean resultant ($\bar{R}$) we use Table A.16 to obtain the corresponding concentration parameter (κ) for directional data in the plane. Alternatively, one can solve the implicit equation for κ given by

$$\bar{R} = \frac{I_1(\kappa)}{I_0(\kappa)}. \tag{A.2}$$

$\bar{R}$	κ	$\bar{R}$	κ	$\bar{R}$	κ
0.00	0.00000	0.34	0.72356	0.68	1.89637
0.01	0.02000	0.35	0.74783	0.69	1.95357
0.02	0.04001	0.36	0.77241	0.70	2.01363
0.03	0.06003	0.37	0.79730	0.71	2.07685
0.04	0.08006	0.38	0.82253	0.72	2.14359
0.05	0.10013	0.39	0.84812	0.73	2.21425
0.06	0.12022	0.40	0.87408	0.74	2.28930
0.07	0.14034	0.41	0.90043	0.75	2.36930
0.08	0.16051	0.42	0.92720	0.76	2.45490
0.09	0.18073	0.43	0.95440	0.77	2.54686
0.10	0.20101	0.44	0.98207	0.78	2.64613
0.11	0.22134	0.45	1.01022	0.79	2.75382
0.12	0.24175	0.46	1.03889	0.80	2.87129
0.13	0.26223	0.47	1.06810	0.81	3.00020
0.14	0.28279	0.48	1.09788	0.82	3.14262
0.15	0.30344	0.49	1.12828	0.83	3.30114
0.16	0.32419	0.50	1.15932	0.84	3.47901
0.17	0.34503	0.51	1.19105	0.85	3.68041
0.18	0.36599	0.52	1.22350	0.86	3.91072
0.19	0.38707	0.53	1.25672	0.87	4.17703
0.20	0.40828	0.54	1.29077	0.88	4.48876
0.21	0.42962	0.55	1.32570	0.89	4.85871
0.22	0.45110	0.56	1.36156	0.90	5.30469
0.23	0.47273	0.57	1.39842	0.91	5.85223
0.24	0.49453	0.58	1.43635	0.92	6.53939
0.25	0.51649	0.59	1.47543	0.93	7.42572
0.26	0.53863	0.60	1.51574	0.94	8.61035
0.27	0.56097	0.61	1.55738	0.95	10.2717
0.28	0.58350	0.62	1.60044	0.96	12.7668
0.29	0.60625	0.63	1.64506	0.97	16.9289
0.30	0.62922	0.64	1.69134	0.98	25.2581
0.31	0.65242	0.65	1.73945	0.99	50.2506
0.32	0.67587	0.66	1.78953	1.00	∞
0.33	0.69958	0.67	1.84177		

Table A.16: Relationship between κ and $\bar{R}$ in 2-D.

ANALYSIS OF DIRECTIONAL DATA

A.9 Critical Values of $\bar{R}$ for 2-D Directional Data

Given the level of significance we determine the critical value for the mean resultant length under the null hypothesis of no preferred direction in the plane ($H_0 : \bar{R} = 0$), with the alternative hypothesis being that the data can be described via the von Mises distribution (9.7) with a preferred trend ($H_1 : \bar{R} \neq 0$).

α:	**0.10**	**0.05**	**0.025**	**0.01**
$n =$ **4**	0.768	0.847	0.905	0.960
5	0.677	0.754	0.816	0.879
6	0.618	0.690	0.753	0.825
7	0.572	0.642	0.702	0.771
8	0.535	0.602	0.660	0.725
9	0.504	0.569	0.624	0.687
10	0.478	0.540	0.594	0.655
11	0.456	0.516	0.567	0.627
12	0.437	0.494	0.544	0.602
13	0.420	0.475	0.524	0.580
14	0.405	0.458	0.505	0.560
15	0.391	0.443	0.489	0.542
16	0.379	0.429	0.474	0.525
17	0.367	0.417	0.460	0.510
18	0.357	0.405	0.447	0.496
19	0.348	0.394	0.436	0.484
20	0.339	0.385	0.425	0.472
21	0.331	0.375	0.415	0.461
22	0.323	0.367	0.405	0.451
23	0.316	0.359	0.397	0.441
24	0.309	0.351	0.389	0.432
25	0.303	0.344	0.381	0.423
30	0.277	0.315	0.348	0.387
35	0.256	0.292	0.323	0.359
40	0.240	0.273	0.302	0.336
45	0.226	0.257	0.285	0.318
50	0.214	0.244	0.270	0.301

Table A.17: Critical values for $\bar{R}$ in the plane. Note the use of n rather than ν.

ANALYSIS OF DIRECTIONAL DATA

A.10 Relationship Between κ and $\bar{R}$ for 3-D Directional Data

Given a mean resultant ($\bar{R}$) we use Table A.18 to obtain the corresponding concentration parameter (κ) for directional data in space. Alternatively, one can solve the implicit equation for κ given by

$$\coth \kappa - 1/\kappa = \bar{R}. \tag{A.3}$$

$\bar{R}$	κ	$\bar{R}$	κ	$\bar{R}$	κ
0.00	0.00000	0.34	1.09951	0.68	3.08456
0.01	0.03000	0.35	1.13739	0.69	3.19091
0.02	0.06001	0.36	1.17584	0.70	3.30354
0.03	0.09005	0.37	1.21490	0.71	3.42314
0.04	0.12012	0.38	1.25459	0.72	3.55051
0.05	0.15023	0.39	1.29497	0.73	3.68655
0.06	0.18039	0.40	1.33605	0.74	3.83232
0.07	0.21062	0.41	1.37789	0.75	3.98905
0.08	0.24093	0.42	1.42053	0.76	4.15819
0.09	0.27132	0.43	1.46401	0.77	4.34143
0.10	0.30182	0.44	1.50839	0.78	4.54076
0.11	0.33242	0.45	1.55372	0.79	4.75857
0.12	0.36315	0.46	1.60005	0.80	4.99772
0.13	0.39402	0.47	1.64745	0.81	5.26167
0.14	0.42503	0.48	1.69599	0.82	5.55463
0.15	0.45621	0.49	1.74573	0.83	5.88181
0.16	0.48756	0.50	1.79676	0.84	6.24971
0.17	0.51909	0.51	1.84915	0.85	6.66652
0.18	0.55083	0.52	1.90300	0.86	7.14279
0.19	0.58278	0.53	1.95842	0.87	7.69228
0.20	0.61497	0.54	2.01550	0.88	8.33333
0.21	0.64740	0.55	2.07437	0.89	9.09091
0.22	0.68009	0.56	2.13515	0.90	10.0000
0.23	0.71306	0.57	2.19799	0.91	11.1111
0.24	0.74632	0.58	2.26304	0.92	12.5000
0.25	0.77990	0.59	2.33049	0.93	14.2857
0.26	0.81381	0.60	2.40050	0.94	16.6667
0.27	0.84806	0.61	2.47331	0.95	20.0000
0.28	0.88269	0.62	2.54914	0.96	25.0000
0.29	0.91771	0.63	2.62825	0.97	33.3333
0.30	0.95315	0.64	2.71093	0.98	50.0000
0.31	0.98902	0.65	2.79751	0.99	100.000
0.32	1.02536	0.66	2.88836	1.00	∞
0.33	1.06218	0.67	2.98389		

Table A.18: Relationship between κ and $\bar{R}$ in 3-D.

ANALYSIS OF DIRECTIONAL DATA

A.11 Critical Values of $\bar{R}$ for 3-D Directional Data

Given the level of significance we determine the critical value for the mean resultant length under the null hypothesis of no preferred direction in space ($H_0 : \bar{R} = 0$), with the alternative hypothesis being that the data can be described via the Fisher distribution (9.31) with a preferred trend ($H_1 : \bar{R} \neq 0$).

α:	**0.10**	**0.05**	**0.025**	**0.01**
$n =$ **5**	0.637	0.700	0.765	0.805
6	0.583	0.642	0.707	0.747
7	0.541	0.597	0.659	0.698
8	0.506	0.560	0.619	0.658
9	0.478	0.529	0.586	0.624
10	0.454	0.503	0.558	0.594
11	0.433	0.480	0.533	0.568
12	0.415	0.460	0.512	0.546
13	0.398	0.442	0.492	0.526
14	0.384	0.427	0.475	0.507
15	0.371	0.413	0.460	0.491
16	0.359	0.400	0.446	0.476
17	0.349	0.388	0.443	0.463
18	0.339	0.377	0.421	0.450
19	0.330	0.367	0.410	0.438
20	0.322	0.358	0.399	0.428
21	0.314	0.350	0.390	0.418
22	0.307	0.342	0.382	0.408
23	0.300	0.334	0.374	0.400
24	0.294	0.328	0.366	0.392
25	0.288	0.321	0.359	0.384
30	0.26	0.29	0.33	0.36
35	0.24	0.27	0.31	0.33
40	0.23	0.26	0.29	0.31
45	0.22	0.24	0.27	0.29
50	0.20	0.23	0.26	0.28
100	0.14	0.16	0.18	0.19

Table A.19: Critical values for $\bar{R}$ in 3-D space. Note the use of n rather than ν.

COURSE REVIEW

Scaling of differential operators in curvilinear coordinates

e.g. In cylindrical coordinates the ***grad*** function is given by

$$\nabla f = \frac{\partial f}{\partial q_1}\hat{\mathbf{h}}_1 + \frac{1}{q_1}\frac{\partial f}{\partial q_2}\hat{\mathbf{h}}_2 + \frac{\partial f}{\partial q_3}\hat{\mathbf{h}}_3.$$

Why does the "q_2" axis have a $1/q_1$ scaling factor?

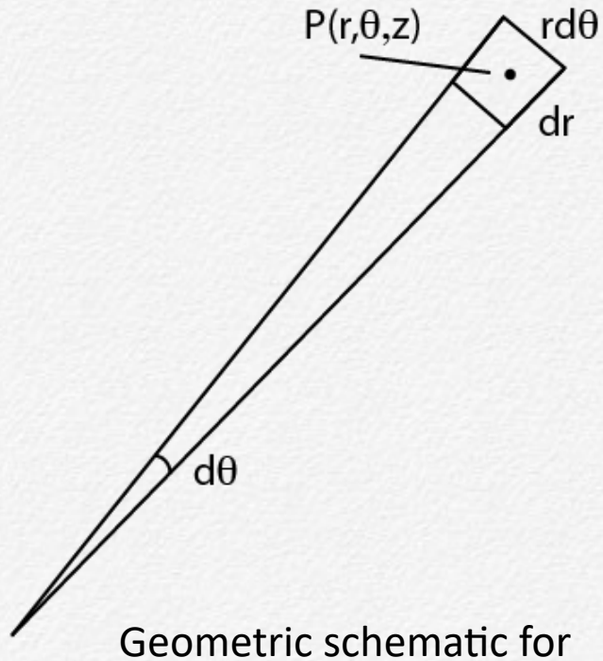

Geometric schematic for differential area in cylindrical coordinates

COURSE REVIEW

grad: vector quantity from a scalar field; components give rate change with respect to each coordinate axis; vector orthogonal to tangent pointing in direction of max change of scalar field at point P (w/ distance); points in the direction of "fastest increase" through the field; magnitude = rate in increase in that direction.

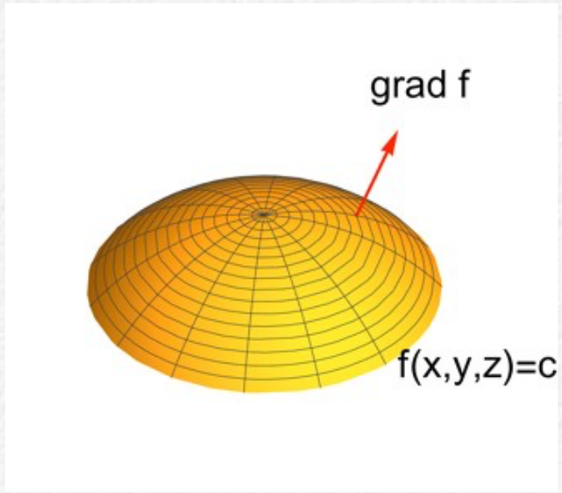

div: scalar quantity from a vector field; sum of the partial derivatives of each component of a field with respect to their coordinate axes. Consider the vector field $\mathbf{v}$ as the velocity field of a streaming fluid. Then this fluid may have sources and sinks. The divergence of the the vector field measures the production- and the destruction rate of the fluid in a given point; the flux generation per unit volume at each point of the field.+ve = source, -ve = sink.

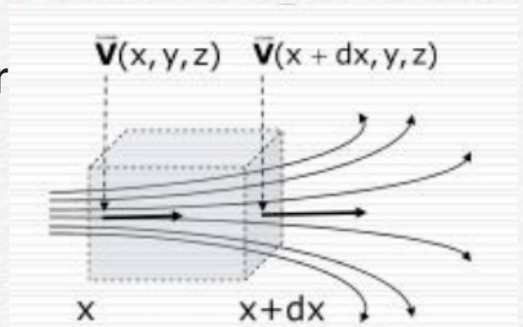

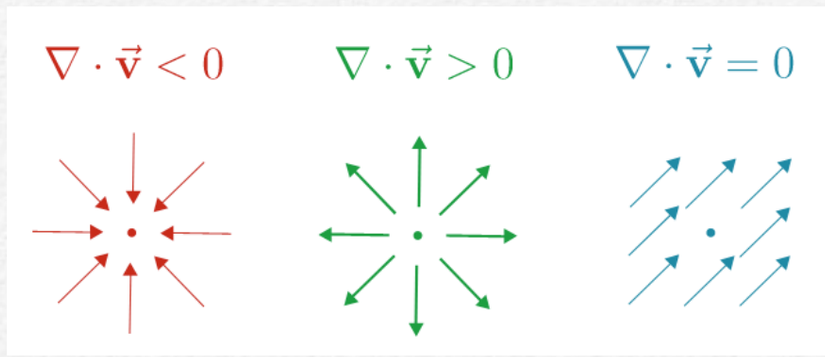

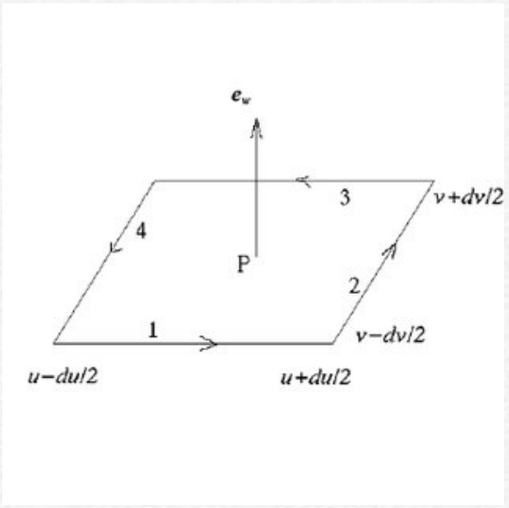

Surface element for the determination of curl's component along w, in curvilinear coordinates

curl: vector quantity from a vector field; vector output that measures "vorticity" at a point with rotation axis oriented along each coordinate axis, so result is perpendicular to coordinate axis; norm = magnitude of rotation.

COURSE REVIEW

Laplacian

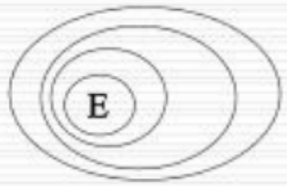

In most of situations, the 2-dimensional Laplacian operator is also related to local minima and maxima. If v_E is positive:

$\Delta\phi = -v_E$: maximum in E (ϕ(E) > average value in the surrounding)

$\Delta\phi = v_E$: minimum in E (ϕ(E) < average value in the surrounding)